Vibrational Spectroscopic Analysis with Chemical Computations for NLO Molecule Benzilic Acid

K.S.BhavaniShamee Ram
Department of Physics and Research Centre, Women's Christian College, Nagercoil, Tamil Nadu 629 001, India
P.Divya
Department of Physics and Research Centre, Women's Christian College, Nagercoil, Tamil Nadu 629 001, India
T.JoselinBeaula
Department of Physics and Research Centre, Women's Christian College, Nagercoil, Tamil Nadu 629 001, India P.
P.Muthuraja
Post graduate and Research Department of Chemistry, Sri Ramakrishna Mission Vidyalaya
College of Arts and Science, Coimbatore - 641020, Tamil Nadu, India
M.Dhandapani
Post graduate and Research Department of Chemistry, Sri Ramakrishna Mission Vidyalaya
College of Arts and Science, Coimbatore - 641020, Tamil Nadu, India
V.BenaJothy*
*Department of Physics and Research Centre, Women's Christian College, Nagercoil, Tamil Nadu 629 001, India

Abstract - Benzilic acid has biological significance and hence is used in the manufacture of glycollate pharmaceuticals including Clidinium, Dilantin, and Flutropium. Experimental findings are added to the quantum chemical studies performed with DFT (B3LYP) method using 6-311+G (d, p) basis sets. Observed FT-IR and FT-Raman spectra have been compared with the theoretical data. Bond length, bond angle and dihederal angle have been calculated using the Gaussian'09 software package wherein experimental values are compared with the theoretical values. Predicted electronic absorption spectrum from TD-DFT calculation has been compared with the UV–vis spectrum. Molecular orbitals and natural bond analysis of the compound have been calculated by Density Functional Theory calculations. HOMO -LUMO energy gap and Molecular Electrostatic Potential values propose the possibility of charge transfer in the molecule.

Index terms: FT-Raman, FT-IR, UV, NMR

1. Introduction

Benzilic acid (C14H12O3) [1], an orthorhombic crystal is used in the manufacture of glycollate pharmaceuticals including Clidinium, Dilantin, and Flutropium, which are antagonists of the muscarinic acetylcholine receptors. It is used in manufacture of the incapacitating agent 3-quinuclidinyl benzilate (BZ) which is regulated by the Chemical Weapons Convention. It is also monitored by law enforcement agencies of many countries, because of its use in the manufacture in hallucinogenic drugs [2]. There has been a growing interest in organic materials for nonlinear optical (NLO) applications in devices such as second harmonic generators, electro-optic modulators, etc. because of their high potential. Organic and polymeric materials have shown great interest in NLO applications [3, 4]. The large nonlinear optical effect found in some organic crystals makes the materials attractive for applications like frequency conversion [5].Organic NLO crystals with aromatic rings have high non-linearity, fast response, tailor-made flexibility, low mobility, large bandgap, high nonlinear coefficients and higher laser damage threshold when compared to inorganic NLO materials [6]

2. Experimental Details

FT-IR and FT-Raman spectra are recorded using PerkinElmer one: FT-IR Spectrometer and Bruker RFS 27: Standalone FT-Raman Spectrometer with resolution of 1 and 2 cm^{-1} respectively. UV–visible absorption spectrum of the sample is measured, using UV–Vis JASCO (V-570) UV/VIS/NIR spectrometer.

3. Computational Details

Density Functional Theoretical (DFT) computations have been enclosed using Gaussian'09 program package [7] at B3LYP/6-311+G (d,p) level. Characterization of normal modes using potential energy distribution (PED) has been performed with MOLVIB - 7.0 written by Sundius [8, 9]. To improve agreement between predicted and observed frequencies, the computed harmonic frequencies have been scaled according to SQMFF procedure [10]. Cartesian representation of force constants have been transferred to non

redundant set of symmetry coordinates, chosen in accordance with the recommendations of Pulay et al. [11].

4. Results and Discussion

4.1 OPTIMIZED GEOMETRY

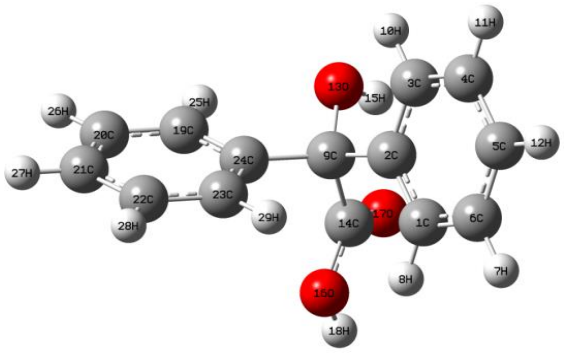

Fig 1: Optimized Structure of Benziic Acid

Optimized geometry of Benzilic aid with numbering scheme of the atoms is presented in Fig1 and optimized structural parameters such as bond length and bond angle along with the compared experimental data are presented in Table1.There are some deviations in the theoretically computed values from the experimental value which may due to the intramolecular interactions in the crystalline state. Structural optimization geometry has been performed at the B3LYP/6-311+G(d, P) basis set for the title compound. Bond lengths C_1-C_6= 1.3955Å, C_2-C_3 = 1.3993Å, C_3-C_4 = 1.3921Å and C_5-C_6 = 1.3917Å is due to the inductive effect caused by electron withdrawing through sigma bond and electron donating through pi bond carbon atoms.[12,13] Bond length C_{14}-O_{16}(1.3424Å) is less than that of persuaded value (1.014Å) [12] due tothe presence of carbonyl group leading to redistributionof electron cloud. It is observed that the influence of the substituent on the molecular parameters, particularly in the C–C bond distance of ring carbon atoms is negligibly small, where the C_{14}-$O_{16}$is in the range of 1.3424-1.014 Å because of the negative oxygen atoms attached to the carbon atoms.

Presence of strong intramolecular hydrogen bond interactions C_{19}-H_{25}…O_{13} and C_3-H_{10}…O_{13} have been confirmed by the measured distances of H_{25}…O_{13} and H_{10}…O_{13} bonds which are 2.40 Å and 2.38 Å, and this length is significantly shorter than the van der Waals separation between the O atom and the H atom lying within the range <3 Å for hydrogen interaction [14]. The C_9-C_2-C_3-C_4 and C_9-C_{14}- O_{16} -H_{18} dihedral angles are 178 and 179 respectively. This is due to the charge delocalization from donor to acceptor group and steric repulsion between the O_{13} and O_{16} atoms [15]

Table1: Optimized Bond lengths (Å), Bond angles (Å) and Dihedral angle(Å)ofBenzilicacidby b3lyp/6-311G(d,p)basis sets

Bond Length	Theo.	Exp.	Bond Angle	Theo.	Exp.	Dihedral angle	Theo.	Exp.
C_2-C_3	1.39	1.42	C_{19}-C_{20}-C_{21}	120.2	121.05	C_1-C_2-C_3-H_{10}	179.3	179.1
C_5-C_6	1.39	1.38	C_{19}-C_{20}-H_{26}	119.5	119.49	C_9-C_{14}-O_{16}-H_{18}	179.5203	175.8
C_{14}-O_{16}	1.3	1.01	C_{21}-C_{20}-H_{26}	120.1	119.46	H_{25}-C_{19}-C_{20}-C_{21}	178.7	177.33
C_{22}-C_{23}	1.39	1.38	C_{20}-C_{21}-C_{22}	119.4	119.08	H_{25}-C_{19}-C_{24}-C_{23}	178.5	177.5
C_{22}-H_{28}	1.08	0.92	C_{20}-C_{21}-H_{27}	120.2	120.47	C_{19}-C_{20}-C_{21}-H_{27}	179.7	178.3
C_{23}-C_{24}	1.39	1.37	C_{22}-C_{21}-H_{27}	120.2	120.45	H_{26}-C_{20}-C_{21}-C_{22}	179.5	178.2
C_{23}-H_{29}	1.08	0.93	C_{21}-C_{22}-H_{28}	120.1	120.45	C_{20}-C_{21}-C_{22}-H_{28}	179.4	177.4
			C_{23}-C_{22}-H_{28}	119.5	120.44	H_{27}-C_{21}-C_{22}-C_{23}	179.7	176.5
			C_{22}-C_{23}-C_{24}	120.4	121.38	C_{21}-C_{22}-C_{23}-H_{29}	179.4	177.6
						H_{28}-C_{22}-C_{23}-C_{24}	179.6	175.6
						C_{22}-C_{23}-C_{24}-C_9	178.3	175.465
						H_{29}-C_{23}-C_{24}-C_{19}	179.2	178.6

5. UV-Visible Spectra

In order to understand electronic transitions, UV–Vis absorption spectrum of PDCA recorded in DMSO is portrayed in Fig. 2.TD-DFT/B3PW91/6-311G (d) calculations havebeen used to determine the low-lying excited states of Benzilic acid. Calculated excitation energies, absorbance and oscillator strength (f) for the Benzilic acid have been compared with the experimental valuesand are tabulated in Table 6. It is contingent from

Fig. 4 that the maximum intensity peak at 266 nm and 235 is mainly due to π-π* transition [16]. Presence of carboxylic acid group and aromatic ring is mainly responsible for π-π* transitions. Electronic transition from the HOMO-1 to LUMO is with 43% contribution, from HOMO to LUMOis with 24% contributionand HOMO to LUMO+1is with 16% contribution.

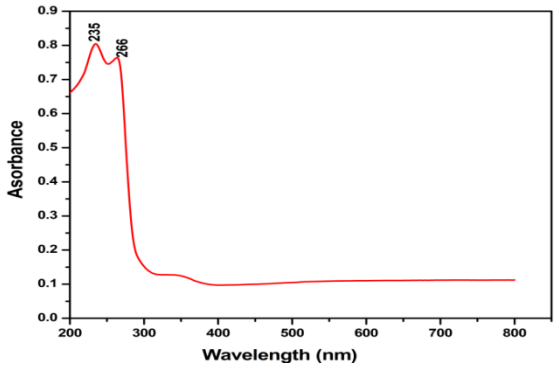

Fig 2: UV-Vis absorption spectrumTable2: UV–vis excitation energy and oscillator strength for Benzilic Acid

Table 5.2: UV–Vis excitation energy and oscillator strength for Benzilic Acid

No.	Energy (cm-1)	Wavelength (nm)		Osc. Strength	Symmetry	Major contribs
		Theo.	Exp.			
1	41092.618	243.3	266	0.022	Singlet-A	H-1->LUMO (44%), HOMO->LUMO (24%), HOMO->L+1 (16%)
2	42104.851	237.5	235	0.002	Singlet-A	H-3->L+1 (15%), H-2->LUMO (38%), H-1->L+1 (10%)
3	42694.447	234.2		0.034	Singlet-A	H-3->LUMO (16%), H-2->LUMO (10%), HOMO->LUMO (34%), HOMO->L+1 (12%)
4	43250.166	231.2		0.040	Singlet-A	H-3->LUMO (12%), H-1->LUMO (39%), HOMO->LUMO (25%)
5	45097.995	221.7		0.0601	Singlet-A	H-3->LUMO (51%), H-2->L+2 (12%)
6	45250.435	220.9		0.0087	Singlet-A	H-3->L+1 (12%), H-2->LUMO (29%), H-1->L+2 (16%)

6.^{13}C NMR Spectra

Appearance of distinct carbon signals in ^{13}C NMRconfirms the molecular structure of the compound. The rangesof^{13}C NMR chemical shifts for organic molecules are observedbetween 0 ppm and 200 ppm [17] and the accuracy ensures reliable interpretation of spectroscopic parameters.^{13}C NMRchemical shifts are tabulated in Table 3.

13C NMR spectrum unambiguously reveals nine distinct carbon signalsindicating different carbon environments present in the compound. Presence of three signals for C_9, C_2, C_{14} is highly deshielded indicating the presence of carboxylic carbon in the compound. Between thesetwo carbonyl carbon signals, the carbon C_9 is highly deshielded, because of its neighborhood electronegative oxygen. Appearance of highintensity signals in the region δ 120–140 ppm indicates the presence of carbons of the aromatic ring. Signal at δ139.77 ppm isassigned to phenyl ring carbon atoms C_1 and $C_4$and the signalat δ133.41 ppm is due to identical aromatic carbons C_4 and C_5respectively. Other aromatic carbon signals appear at δ130.24, δ124.09and δ126.59 ppm for $C_{19,22}$, $C_{23,24}$ and $C_{20,21}$ respectively.

Table 3: Absorbed and predicted ^{13}C NMR Spectra Spectra isotropic chemical shift for benzilic acid

Atom (^{13}C)	Theoretical	Experimental
C_1	148.3515	139.77
C_2	166.4376	166.76
C_3	150.0509	148.6
C_4	152.0603	139.77
C_5	150.8884	133.41
C_6	149.962	133.41
C_9	102.9253	40.56
C_{14}	200.0158	168.18
C_{19}	149.1016	130.24
C_{20}	150.2236	126.57
C_{21}	150.7114	126.57
C_{22}	140.3363	130.24
C_{23}	152.3412	124.09
C_{24}	152.3412	124.09

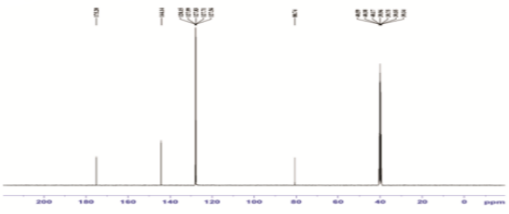

Fig 3: ^{13}C NMR spectra of Benzilic acid

7. ^{1}H NMR spectra

Hydrogen atoms are mostly localized on the periphery of the molecules and their chemical shifts would be more susceptible to intramolecular interactions in the aqueous solutions as compared to that for other heavier atoms. Signals of aromatic protons are observed between 2-13 ppm and proton signal is deshielded for H_{26} and H_{29} due to the carboxylic group as observed at 7.315 ppm.

Table 4: Absorbed and predicted ^{1}H NMR Spectra isotropic chemical shift for benzilic acid

Atom (^{1}H)	Theoretical	Experimental
H7	8.4874	13.25
H8	8.9655	7.404
H10	8.9221	13.25
H11	8.4762	13.24
H12	8.3822	13.24
H15	4.5432	2.511
H18	7.6804	2.511
H25	8.9579	6.364
H26	8.4405	7.315
H27	8.3272	7.298
H28	8.252	7.298
H29	7.9239	7.315

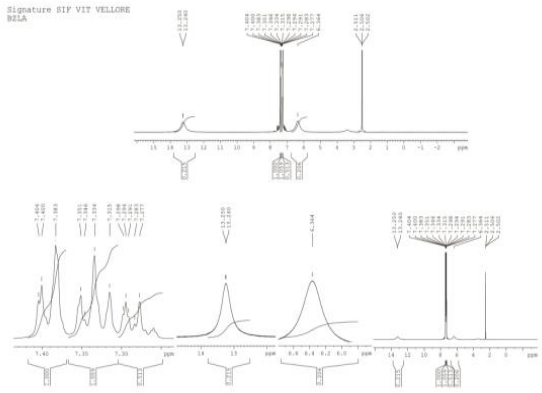

Fig 4: 1H NMR spectra of Benzilic acid

8. VIBRATIONAL SPECTRAL ANALYSIS

8.1 Phenyl ring vibrations

Aromatic structure shows the presence of C−H stretching vibrations in the characteristic region 3100−3000 cm^{-1} [18]. For the title compound, these bands were observed at 3059 cm^{-1} and 3073 cm^{-1} in FT-IR and FT-Raman spectra respectively. Intensity of the FT-IR spectral band at 3059 cm^{-1} is very small, and this striking discrepancy is due to the formation of intramolecular C-H…O interaction. Since the bands are mixed in a very broad profile, thebands observed are very weak shoulderin that region. Theoretically computed values for C-H stretching vibrations are scaled at 3069 and 3066cm^{-1} with 75-99% contribution in PED.C-H in-plane bending vibrations normally occurs as a strong to weak intense bands in the region 1000–1520cm^{-1}[19,20]. The C−H in-plane bending vibrations of the compound are computed at1322, 1168 cm^{-1} in FT−IR and 1171 cm^{-1} in FT−Raman.

C–C stretching frequencies are generally predicted in the region 650–1650 cm^{-1} [21, 22]. Several ring modes are affectedby substitution in the aromatic ring: with heavy substituents, thebands tend to shift somewhat to lower wavenumbers and greater the number of substituents on the ring, broader is theabsorption region [19,20]. Weak and strong bands of C-C stretching vibrations are observed at 1608in FT-Raman and at 1619, 1488 and 1435 cm^{-1} in FT-IR with the scaled values at 1621, 1497, 1454 and 1618 cm^{-1} where these modes are pure stretching modes as manifested from the PED value 40-70%.

8.2 Carboxylic acid group vibrations

Vibrational analysis of carboxylic acid was carried out giving preferences to carbonyl and hydroxyl groups wherein stretching vibrations are generally observed in the regionaround3500 cm^{-1}[23]. Most important spectral feature of COOH group is -OH hydroxyl group that connects the molecules and is likely to be more sensitive to the environment which causes pronounced shifts in the hydrogen-bonded species. Weak and very strong bands observed at 3387in FT-IR and at 3390 cm^{-1} in FT-Raman are assigned to O-H stretching vibration. Theoretically predictedwavenumbers (3385cm^{-1}and 3387cm^{-1}) coincide exactlywith the experimental wavenumbers and these modes are purestretching modes as evident from the PED value (93 and 100 %).

Carbonyl stretching C=O vibration [24] expected in the region1715-1680 cm^{-1}, appears at1708cm^{-1}and 1710 cm^{-1} in FT-IR and FT-Raman spectra while PED calculations locate it at1720 cm^{-1}. Formation of hydrogen bondscan increases the intensity of the carbonyl group because of conjugation and so conjugationleads to the intensification of Raman aswell as the infrared band intensities. C=O stretching mode is found to be simultaneously activein both IR and Raman spectra.

InfraredandRamanspectra arecomplementaryinmost cases and so the strongestband in the Raman spectrum is weak in the IR spectrum and vice versa

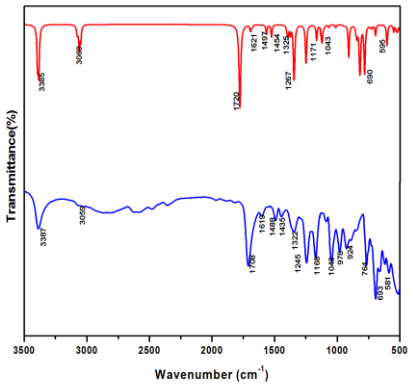

Fig 5a: Experimental and stimulated FT-IR spectra of Benzilic acid

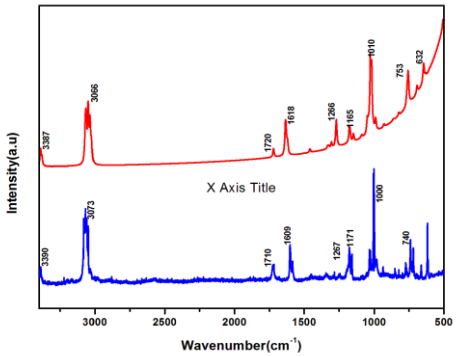

Fig 5b: Experimental and stimulated FT-Raman spectra of Benzilic acid

9. NBO Analysis

NBO analysis has been performed to identify and confirm the possible intra and intermolecular interactions between units that will form proper and improper hydrogen bonding [25]. Electronic interactions within these orbitals, deviation from Lewis electronic structure and delocalization effect can be interpreted as charge transfer between filled Lewis orbitals (donors) and theoretically empty non-Lewis orbitals (acceptors). Magnitude of these delocalization effects can be determined from an analysis of the off diagonal elements in Fock matrix of NBO basis by taking into account all possible donor–acceptor interactions and then by calculating strength of them by second order theory. Second-order perturbation theory of Fock matrix in NBO shows strong intramolecular hyperconjugative interaction which are presented in Table 5.

Table 5: Second order perturbation theory analysis of Fock matrix in NBO analysis

Donor (i)	ED(i)(e)	Acceptor (j)	ED (j) (e)	E (2)[a] (kJ mol-1)	E (j)-E(i)[b] (a.u)	F (i,j) [c] (a.u)
πC_1-C_2	1.67135	π^* C_3-C_4 π^* C_5-C_6	0.31008 0.32669	19.50 19.98	0.29 0.29	0.068 0.068
πC_3-C_4	1.65383	π^* C_1-C_2 π^* C_5-C_6	0.35583 0.32669	21.16 20.83	0.28 0.28	0.069 0.068
σC_5-C_6	1.97950	π^* C_1-C_2 π^* C_3-C_4	0.35583 0.31008	20.41 19.53	0.28 0.29	0.068 0.067
πC_{19}-C_{20}	1.65754	π^* C_{21}-C_{22} π^* C_{23}-C_{24}	0.33052 0.35039	20.81 20.60	0.28 0.28	0.068 0.068
π C_{21}-C_{22}	1.66286	π^* C_{19}-C_{20} π^* C_{23}-C_{24}	0.31706 0.35039	19.74 20.71	0.28 0.29	0.067 0.069
π C_{23}-C_{24}	1.65985	π^* C_{19}-C_{20} π^* C_{21}-C_{22}	0.31706 0.33052	20.33 19.96	0.29 0.28	0.068 0.067
LP_2-O_{16}	1.81459	σ^*C_{14}-O_{17}	0.02164	46.45	0.35	0.114
LP_2-O_{17}	1.84203	σ^*C_9-C_{14} σ^*C_{14}-O_{16}	0.09097 0.09099	18.76 30.98	0.62 0.63	0.098 0.127

E(2)[a] means energy of hyper conjugative interaction

E (j)-E(i)[b] Energy difference between donor and acceptor i and j NBO orbitals

F (i,j) [c] is the Fock matrix element between i and j NBO orbitals

Intramolecularhyperconjugative interactions are formed by the orbital overlap between $\pi(C_1$-$C_2)$, π $(C_3$-$C_4)$, π $(C_{19}$-$C_{20})$, π $(C_{21}$-$C_{22})$ π $(C_{23}$-$C_{24})$ and π^* $(C_3$-$C_4)$, π^* $(C_5$-$C_6)$, $\pi^*($ C_1-$C_2)$, π^* $(C_5$-$C_6)$, π^* $(C_{21}$-$C_{22})$, $\pi^*($ C_{23}-$C_{24})$, π^* $(C_{19}$-$C_{20})$, π^* $(C_{23}$-$C_{24})$, π^* $(C_{19}$-$C_{20})$, π^* $(C_{21}$-$C_{22})$ bond orbitals which results in intramolecular charge transfer (ICT) causing stabilization of the system [26,27]. This strong ICT is one of the causes of the NLO activity. Energy contribution of $LP_2O_{16} \rightarrow \sigma^*(C_{14}$–$O_{17})$,$LP_2O_{17} \rightarrow \sigma^*(C_9$–$C_{14})$, $LP_2O_{17} \rightarrow \sigma^*(C_{14}$–$O_{16})$, values are 46.45, 18.76 and 30.98 kcal mol^{-1}respectively. This increase in hyperconjugative interaction energies compared to that of other lone pair interaction energies gives evidence for resonance and this is due to the presence of electron donating oxygen atoms. Strengthening and contraction of C–H bonds is due to rehybridization, [28] which is revealed by the low value of electron density (0.01476e, 0.01380e) in $\sigma^*(C_3$-$H_{10})$ and σ^* $(C_6 - H_7)$ orbitals, respectively**.**

10. HOMO LUMO ANALYSIS

The highest occupied molecular orbitals (HOMOs) and lowest unoccupied molecular orbitals (LUMOs) play an important

role in the optical and electronic properties. The HOMO energy characterizes the ability of electron giving; LUMO energy characterizes the ability of electron accepting [29]. Recently,energy gap between HOMOand LUMO has been used to prove bioactivity from intramolecular charge transfer [30,31,32].

HOMO, of π nature (i.e., aromatic ring), is delocalized over whole C– C bond and LUMO is located over aromatic ring. Consequently, HOMO-LUMO transition implies an electron density transfer to COOH and OCH3 group from the aromatic ring [33].

Calculated energies and energy gap are:

HOMO energy = -6.594681eV

LUMO energy = -0.9823314eV

Band gap energy =-5.612350eV

Lower HOMO–LUMOenergy gap shows the possibility of intramolecular charge transferanalysis and confirms the bioactivity of the molecule. Molecularorbital plots of the frontier orbitals for the ground state of Benzilic Acid molecule including HOMO and LUMO are shown in Fig.6a & 6b

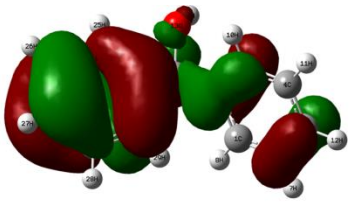

Fig 6a: HOMO

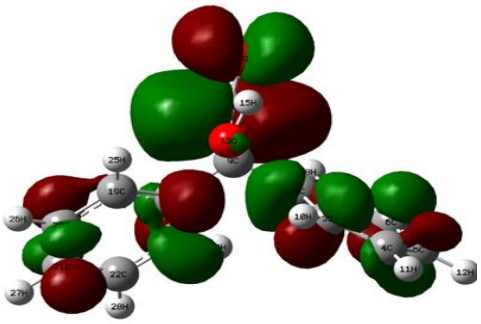

Fig 6b: LUMO

11. MOLECULAR ELECTROSTATIC POTENTIAL (MEP)

3D plot of molecular electrostatic potential of the title compound by B3LYP/6-311+G (d,p) is shown in Fig 7.MEP is a plot of electrostatic potential mapped onto the constant electron density surface and simultaneously displays the molecular size, shape and electrostatic potential value in terms of color coding. MEP is employed to distinguish regions on the surface which are electron poor (electrophilic attack) from those which are electron rich nucleophilicattack).

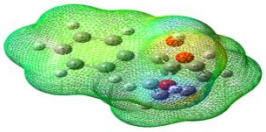

Fig 7: Molecular electrostatic potential map of Benzilic acid calculated at B3LYP/6-311+G(d,p)

Different values of the electrostatic potential at the surface are represented by different colors; red represents the region of the most electronegative electrostatic potential, blue represents the region of the most positive electrostatic potential, green represents the region of zero potential and yellow represents slightly electron rich region [34]. FromFig 3 it is seen that negative regions are associated with the lone pair of oxygen atoms, showing red colour indicating the site is rich in negative potential, while the blue colour indicates the site is rich in positive potential due to the presence of the hydrogen atoms. Strongest attraction will be seen in the nucleophilic site due to the balancing of both hydrogen and lone pair atoms. Strongest repulsion will be seen in the electrophilic site due to the presence of abundant positive atoms [35]. From MEP studies it is found that the distribution of the charge will be in the range of -7.345e-2 and 7.345e-2.This figure provides a visual representation of the chemically active sites and comparative reactivity of atoms.

12. Conclusion

Detailed analyses of the spectroscopic parameters using quantum chemical computations have been performed for the title compound.Molecular geometry analysis of benzilicacidshowsslight variations in the bond lengths of C_1-C_6= 1.3955Å, C_2-C_3 = 1.3993Å, C_3-C_4 = 1.3921Å and C_5-C_6 = 1.3917Å which is due to the inductive effect caused by electron withdrawing through sigma bond and electron donating through pi bond carbon atoms. UV analysis reveals that π-π^* transitions is due to the presence of carboxylic acid group and aromatic ring.[13]C NMR spectral analysis indicates thatcarbon C_9 is highlydeshielded, because of its

neighborhood electronegative oxygen.MEP has been performed to distinguish regions on the surface which are electron poor and electron rich.

REFERENCES

[1] Yongcai Qiu, Kunnam Wang, Yan Liu, Hong Deng, Feng Sun, YuepengCai, (2007) J. Inorg. Chem. Act 360, 1819
[2] Nerve Agent Precursers "Benzilic acid and Methyl Benzilate" Factsheets on Chemical and Biological Warefare Agents, Chemical precursors.
[3] Prasad P.N., Williams D.J. (1991) "Introduction to Nonlinear Optical Effects in Molecules and Polymers" Wiley, New York.
[4] Chemla D.S., Zyss J. (1987), "Nonlinear Optical Properties of Organic Molecules and Crystals" Academic, New York
[5] Maloney C., Blau W. (1987), J. Opt. Soc. Am. B 14 1035.
[6] Gopalakrishnan R., Ramasamy P.(2004), "Proceedings of the international workshop on crystal growth and characterization of technologically important materials" Chennai, India, p. 23.
[7] M. J. Frisch et al., Gaussian 09, Revision D.01, Gaussian, Inc.,Wallingford CT, (2010)
[8] T. Sundius, Vib. Spectrosc. 29 (2002) 89–95.
[9] T. Sundius, J. Mol. Struct. 218 (1990) 321.
[10] P. Pulay, G. Fogarasi, G. Pongor, J.E. Boggs, A. Vargha, J. Am. Chem. Soc. 105(1983) 7037.
[11] P. Pulay, G. Fogarasi, F. Pang, J.E. Boggs, J. Am. Chem. Soc. 101 (1979) 2550
[12] M. Joseph, Hornback, University of Denver, Organic Chemistry, 2006, p. 94.
[13] R.D. Harcourt, Qualitative Valence-Bond Descriptions of Electron-Rich Molecules: Pauling '3-ElectronBonds' and Increased-Valence'Theory, Springer-Verlag, Berlin Heidelberg, 1982, p. 121
[14] A. Bondi, J. Phys. Chem. 68 (1964) 441
[15] Growth, electronic absorption and vibrational spectral analysis of semiorganic nonlinear optical material potassium acid phthalate: A scaled quantum mechanical force field study S. Alena,b , D. Sajan , N. Vijayan c , K. Chaitanya d , Ivan Ne˘mec e , V. BenaJothy
[16] P. Muthuraja, M. Sethuram, M. Sethu Raman, M. Dhandapani, G. Amirthaganesan, J. Mol. Struct. 1053 (2013) 5-14.
[17] Neil E. Jacobsen, NMR Data Interpretation Explained: Understanding 1d and 2D NMR Spectra of Organic Compounds and Natural Products, Wiley 2016.
[18] S. Mohan, V. Illangovan, Indian J. Pure Appl. Phys. 31 (1993) 750–754
[19] L.J. Bellamy "The Infra-red Spectra of Complex Molecules" Chapman and Hall Ltd., London, 1975.
[20] G. Varsanyi, Assignments for Vibrational Spectra of Seven Hundred Benzene Derivatives, vols. 1and 2, Adam Hilger, 1974.
[21] N.P.G. Roeges "A Guide to Complete Interpretation of Infrared Spectra of Organic Structures" Wiley, New York, 1994.
[22] G. Socrates, Infrared Characteristic Group Frequencies, Wiley-Inter Science Publication, New York, 1990.
[23] D. Michalska, D.C. Bienko, A.J.A. Bienko, Z. Latajaka, J. Phys. Chem. 100 (1996) 17786–17790.
[24] Jag Mohan, Organic Spectroscopy: Principles and Applications, Alpha Science International Ltd., Harrow, UK, (2002) 60.
[25] Jana Chocholousova, Vladimir Spirko, PavelHobza, Phys. Chem. Chem. Phys. 6 (2004) 37–41
[26] F. Weinhold, Chemistry: a new twist on molecular shape, Nature 411 (2001) 539–541.
[27] F. Weinhold, C. Landis, Valency and Bonding: A Natural Bond Orbital Donor–Acceptor Perspective, Cambridge University Press, Cambridge, 2005
[28] I. V. Alabugin, M. Manoharan, S. Peabody and F. Weinhold, J. Am. Chem. Soc., 2003, 125, 5973–5987
[29] M. Karabacak, E. Kose, A. Atac, Spectrochim. Acta. 91A (2012) 83–96.
[30] M. Kurt, P. ChinnaBabu, N. Sundaraganesan, M. Cinar, M. Karabacak, Spectrochim. Acta Part A 79 (2011) 1162–1170.
[31] L. Padmaja, C. Ravikumar, D. Sajan, I.H. Joe, V.S. Jayakumar, G.R. Pettit, O.F. Nielsen, J. Raman Spectrosc. 40 (2009) 419–428.
[32] C. Ravikumar, I.H. Joe, V.S. Jayakumar, Chem. Phys. Lett. 460 (2008) 552–558
[33] R. G. Pearson, "Absolute electronegativity and absolute hardness of Lewis acids and bases," Journal of the American Chemical Society, vol. 107, no. 24, pp. 6801–6806, 198
[34] T.Chithambarathanu, K.Vanaja and J.DaisyMagdalin "Molecular Structure, Spectroscopic studies,homo-lumo profile and NBO analysis of 3-Ethoxy-4-hydroxy benzaldehyde. (504)
[35] T.JoslinBeaula, A.Packiavathi, D.Manimaran, I. Hubert Joe, V.K. Rastogi, V.BenaJothy "Quantum chemical computations, vibrational spectroscopic analysis and antimicrobial studies of 2, 3-Pyrazinedicarboxylic acid